Covariance analysis for evaluating head trackers

Donghoon Kang*
Korea Institute of Science and Technology, Imaging Media Research Center, Seoul, Republic of Korea

Abstract. Existing methods for evaluating the performance of head trackers usually rely on publicly available face databases, which contain facial images and the ground truths of their corresponding head orientations. However, most of the existing publicly available face databases are constructed by assuming that a frontal head orientation can be determined by compelling the person under examination to look straight ahead at the camera on the first video frame. Since nobody can accurately direct one's head toward the camera, this assumption may be unrealistic. Rather than obtaining estimation errors, we present a method for computing the covariance of estimation error rotations to evaluate the reliability of head trackers. As an uncertainty measure of estimators, the Schatten 2-norm of a square root of error covariance (or the algebraic average of relative error angles) can be used. The merit of the proposed method is that it does not disturb the person under examination by asking him to direct his head toward certain directions. Experimental results using real data validate the usefulness of our method. [DOI: 10.1117/1.OE.56.10.103105]

Keywords: head orientation; covariance; uncertainty; evaluation.

Paper 171111L received Jul. 20, 2017; accepted for publication Sep. 21, 2017; published online Oct. 13, 2017.

1 Introduction

The performance of head orientation tracking algorithms (i.e., head trackers) with cameras is commonly evaluated by using publicly available face databases.[1–3] This is because face databases contain the information about the ground truths of head orientations as well as facial images. To collect the ground truths of head orientations, a checkerboard or an optical motion capture system is usually used. When attaching a checkerboard (or reflective markers) to a person's head, one may find that it is unavoidable to have a rotational mismatch between the head frame $\{E\}$ in Fig. 1(a) and the checkerboard frame (or reflective marker frame) $\{A\}$ in Fig. 1(b).

To resolve the issue of this rotational mismatch, existing publicly available face databases mostly assume that a frontal head orientation can be determined by compelling the person under examination to look straight ahead at the camera on the first video frame.[4–9] Since nobody can accurately direct one's head toward the camera, this assumption may be unrealistic. To correctly evaluate the performance of head trackers, this assumption should be discarded. In contrast, the ground truth positions of an eye as a particular point on the head can be obtained without the above assumption by using a recent method.[10]

Rather than obtaining estimation error angles by directly comparing the outputs of head trackers with their corresponding ground truths, one may consider computing the "error covariance" to evaluate the performance of head trackers in terms of estimation "uncertainty."[11–13] Unfortunately, most of the existing methods for computing the error covariance also assume that the relative rotation between the head frame $\{E\}$ and the pattern frame $\{A\}$ in Fig. 1 is given, but it is actually unknown. As we point out at the above paragraph, this assumption is unrealistic and should be removed. In this paper, we present a method for evaluating the uncertainty of head trackers by computing the covariance of error rotations without compelling the person under examination to look straight ahead in order to set the frontal head orientation. If the Schatten 2-norm of a square root of error covariance (or the algebraic average of relative error angles) is used as an uncertainty measure of estimators, then a smaller value of this norm is preferable as a reliable estimator.

The remainder of this paper is organized as follows. In Sec. 2, we establish some notation and provide mathematical preliminaries. The problem statement is given in Sec. 3. In Sec. 4, we present a method for computing the covariance of estimation errors and two measures for evaluating the uncertainty of estimators. Experimental results using real data sets are presented in Sec. 5 to demonstrate the usefulness of the proposed method.

2 Mathematical Preliminaries

We first establish some notations and provide useful equations involving the rotation group, denoted $SO(3)$.[14,15] $SO(3)$ is an example of matrix Lie group and consists of 3×3 orthogonal matrices with determinant 1. The Lie algebra of $SO(3)$, denoted $so(3)$, is the set of 3×3 skew-symmetric matrices of the form

$$[\mathbf{r}] := \begin{bmatrix} 0 & -r_3 & r_2 \\ r_3 & 0 & -r_1 \\ -r_2 & r_1 & 0 \end{bmatrix},$$

where $\mathbf{r} = (r_1, r_2, r_3)^{\mathrm{T}} \in \mathbb{R}^3$. In this paper, we use the square bracket $[\mathbf{r}] \in so(3)$ to denote the skew-symmetric matrix representation of a vector $\mathbf{r}$.

The exponential mapping $\exp : so(3) \to SO(3)$ is given by the following explicit equation. Given $[\omega] \in so(3)$

$$\exp[\boldsymbol{\omega}] = \mathbf{I}_3 + a[\boldsymbol{\omega}] + b[\boldsymbol{\omega}]^2 \in SO(3),$$

*Address all correspondence to: Donghoon Kang, E-mail: kimbab.moowoo@gmail.com

where $\mathbf{I}_3$ is the 3×3 identity matrix, $a=(\sin\|\boldsymbol{\omega}\|)/\|\boldsymbol{\omega}\|$, and $b=(1-\cos\|\boldsymbol{\omega}\|)/\|\boldsymbol{\omega}\|^2$. The inverse of the exponential map or logarithm can also be expressed as follows. Suppose $\mathbf{R}\in SO(3)$ such that $\mathrm{tr}(\mathbf{R})\neq -1$, where $\mathrm{tr}(\cdot)$ denotes the trace of a matrix. Thus

$$\log\mathbf{R}=\frac{\theta}{2\sin\theta}(\mathbf{R}-\mathbf{R}^{\mathrm{T}}),$$

where θ satisfies $1+2\cos\theta=\mathrm{tr}(\theta)$, $|\theta|<\pi$, and $\|\log\mathbf{R}\|/\sqrt{2}=\theta$. Here, $\|\cdot\|$ denotes the Frobenius norm. If $\mathrm{tr}(\mathbf{R})=-1$, then the logarithm $[\mathbf{r}]:=\log\mathbf{R}$ has two antipodal solutions $\pm\mathbf{r}$, which can be determined from the relation $\mathbf{R}=\mathbf{I}_3+(2/\pi^2)[\mathbf{r}]^2$.

3 Problem Statement

In this paper, we will call the frame fixed to a head as the "head frame." Let $\mathbf{G}_k\in SO(3)$ denote the estimate of head orientation at time instant k provided by a certain head orientation tracker as depicted in Fig. 1(a). Since every head tracker defines its own frame $\{E\}$ fixed to a particular point on the head, $\mathbf{G}_k$ represents the estimated orientation of the head frame $\{E\}$ with respect to the camera frame $\{C\}$, which can be compactly rewritten as $\mathbf{G}_k:\{C\}\rightarrow\{E\}$ [see Fig. 1(a)].

To evaluate the performance of head trackers, we need the accurate information about head orientations, which is commonly called as the "ground-truths" of head orientations. Let $\mathcal{G}_k\in SO(3):\{C\}\rightarrow\{E\}$ be the ground-truth of $\mathbf{G}_k$ at time instant k. The error of $\mathbf{G}_k$, denoted $\delta\mathbf{G}_k\in SO(3)$, can be defined as

$$\delta\mathbf{G}_k:=\mathbf{G}_k^{-1}\mathcal{G}_k. \tag{1}$$

Thus, the goal of this paper is to approximate the covariance of error rotations $\{\delta\mathbf{G}_1,\ldots,\delta\mathbf{G}_N\}$, denoted $\mathbf{P}$, where N is the number of measurements.

4 Method

4.1 *Ground-Truths of Head Orientations*

To obtain $\mathcal{G}_k$ at time step k, one may consider using a checkerboard pattern as shown in Fig. 1(b). Using a standard method[16] for camera calibration, we can obtain $\mathbf{D}_k\in SO(3):\{C\}\rightarrow\{A\}$. From Fig. 1(b), $\mathcal{G}_k$ can be given by

$$\mathcal{G}_k=\mathbf{D}_k\mathbf{W},\quad (k=1,\ldots,N), \tag{2}$$

where $\mathbf{W}\in SO(3):\{A\}\rightarrow\{E\}$ is an unknown and "constant" transformation.

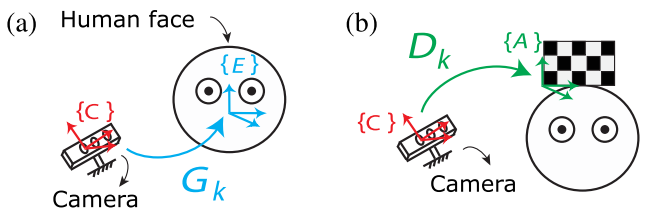

Fig. 1 System setups for collecting head orientations. (a) Original system and (b) using a checkerboard.

Algorithm 1 Rotation averaging.

Input: a set of rotation matrices $\{\mathbf{B}_1,\ldots,\mathbf{B}_N\}$

$\mathbf{T}\leftarrow\mathbf{B}_1$

for $k\leftarrow 0$ **to** M **do**

$\Lambda\leftarrow\frac{1}{N}\sum_{k=1}^{N}\log(\mathbf{B}_k\mathbf{T}^{-1})$

$\mathbf{T}\leftarrow\exp(\Lambda)\mathbf{T}$

end

return T

4.2 *Covariance of Estimation Errors*

By substituting Eq. (2) into Eq. (1), we have

$$\delta\mathbf{G}_k:=\mathbf{B}_k\mathbf{W}, \tag{3}$$

where $\mathbf{B}_k:=\mathbf{G}_k^{-1}\mathbf{D}_k\in SO(3)$. Let $\bar{\mathbf{B}}\in SO(3)$ denote the average rotation matrix of $\mathbf{B}_1,\ldots,\mathbf{B}_N$. Using Algorithm 1,[17] $\bar{\mathbf{B}}$ can be obtained. Since Algorithm 1 converges rapidly,[18] it is enough to set $M=4$. Thus, $\mathbf{B}_k$ can be modeled as

$$\mathbf{B}_k=\exp[\xi_k]\bar{\mathbf{B}}, \tag{4}$$

where $[\xi_k]\in so(3)$. Given $\mathbf{B}_k$ and $\bar{\mathbf{B}}$, we can compute ξ_k by

$$[\xi_k]=\log(\mathbf{B}_k\bar{\mathbf{B}}^{-1}). \tag{5}$$

When substituting Eq. (4) into Eq. (3), we can obtain

$$\delta\mathbf{G}_k=\exp[\xi_k]\bar{\mathbf{B}}\mathbf{W}.$$

Since $\mathbf{W}$ is constant, the average of $\delta\mathbf{G}_1,\ldots,\delta\mathbf{G}_N$ is $\bar{\mathbf{B}}\mathbf{W}$. By combining the ideas of recent works,[19,20] the "covariance" of error rotations $\delta\mathbf{G}_1,\ldots,\delta\mathbf{G}_N$ can be approximated by

$$\mathbf{P}=\frac{1}{N}\sum_{k=1}^{N}\xi_k\xi_k^{\mathrm{T}}. \tag{6}$$

Let the singular value decomposition (SVD) be given by $\mathbf{P}=\mathbf{U}\mathbf{S}\mathbf{U}^{\mathrm{T}}$, where $\mathbf{U}$ is an orthogonal matrix and $\mathbf{S}$ is a diagonal matrix. Thus, the square root of $\mathbf{P}$ is given by $\sqrt{\mathbf{P}}=\mathbf{U}\sqrt{\mathbf{S}}\mathbf{U}^{\mathrm{T}}$. If the singular values of $\sqrt{\mathbf{P}}$ are denoted by $r_1,r_2,r_3>0$, then one may use

$$\epsilon:=\left(\sum_{m=1}^{3}r_m^2\right)^{1/2}, \tag{7}$$

as an uncertainty measure of estimators. In mathematics, ϵ in Eq. (7) is called the Schatten 2-norm of $\sqrt{\mathbf{P}}$. In this paper, we choose the Schatten 2-norm of $\sqrt{\mathbf{P}}$ as an uncertainty measure of estimators because its physical meaning can be intuitively understood as follows. The Schatten 2-norm of $\sqrt{\mathbf{P}}$ is the square root of the sum of lengths squared in the direction of the principal axes of the error ellipsoid. Recall that the value of the Frobenius norm is equal to that of the Schatten 2-norm (see Appendix A). As an alternative uncertainty measure of estimators, one can use

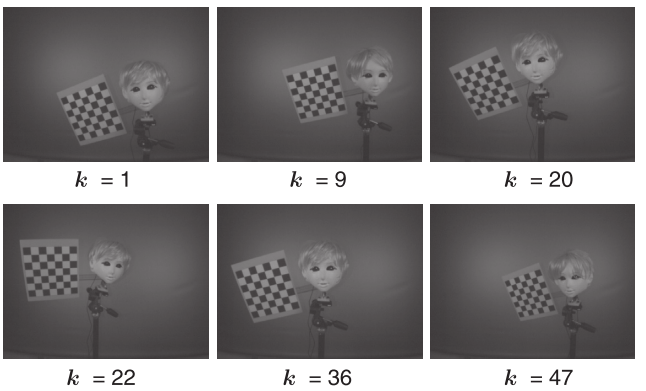

Fig. 2 Images of a mockup face and a checkerboard captured by an infrared camera in the Intel RealSense™ F200.

$$\gamma := \frac{1}{N}\sum_{k=1}^{N} \|\xi_k\|. \tag{8}$$

As ϵ (or γ) becomes large, the uncertainty of an estimator also increases. For this reason, a smaller ϵ (or γ) is preferable as a reliable estimator.

5 Experimental Results

We perform real experiments for evaluating the performances of two different head tracker systems by using the proposed method.

- In the first experiment, we evaluate the performance of a head tracker system consisting of the Intel RealSense™ F200 RGB-D (red, green, blue, and depth) camera and Intel RealSense™ Software Development Kit (SDK), version 2015 R5.
- The second experiment is conducted for evaluating the performance of a more recent version of the head tracker system, which includes Intel RealSense™ SR300 RGB-D camera and Intel RealSense™ SDK, 2016 R2.

5.1 *First Experiment by Using the Intel RealSense™ F200 RGB-D Camera and the SDK 2015 R5*

5.1.1 *Norms of noises*

To emulate a person's face in Fig. 1(b), we use a mockup face. As shown in Fig. 2, we attach a 7×7 checkerboard to the mockup face, of which checker square is of dimension 40 mm $\times$ 40 mm.

While keeping a mockup face stationary for a moment at the k'th experiment, we can collect a set of data $\{\mathbf{H}_k^{(1)}, \ldots, \mathbf{H}_k^{(N_t)}\} \subset SO(3)$, which is provided by the head tracker system. In each experiment, $N_t = 30$. In this situation, the infrared camera in the Intel RealSense™ F200 RGB-D camera fixed to the ground captures the image of the checkerboard attached to the mockup face as shown in Fig. 2. Let $\mathbf{D}_k$, depicted in Fig. 1(b), be the average of rotation matrices $\{\mathbf{H}_k^{(1)}, \ldots, \mathbf{H}_k^{(N_t)}\}$, which can be obtained by using Algorithm 1. In a similar fashion to Eq. (4), we can model $\mathbf{H}_k^{(j)}, (j = 1, \ldots, N_t)$ as $\mathbf{H}_k^{(j)} = \exp[\eta_k^{(j)}]\mathbf{D}_k$, where $\eta_k^{(j)}$ denotes the noise vector at the time step j in the k'th experiment. Using the equation, $[\eta_k^{(j)}] = \log[\mathbf{H}_k^{(j)}\mathbf{D}_k^{-1}] \in so(3)$, we can obtain $\eta_k^{(j)}$. In a similar way to Eqs. (6) and (7), $f_k \in \mathbb{R}$ at the k'th experiment can be defined by

$$f_k := \frac{180 \text{ deg}}{\pi}\left(\sum_{m=1}^{3} u_m^2\right)^{1/2}, \tag{9}$$

where $u_1, u_2, u_3 > 0$ are the singular values of $\sqrt{\mathbf{Q}_k}$. Here, $\mathbf{Q}_k = \sum_{j=1}^{N_t} \boldsymbol{\eta}_k^{(j)} \boldsymbol{\eta}_k^{(j)\mathrm{T}}$ represents the noise covariance at the k'th experiment. The physical meaning of Eq. (9) is that f_k is the norm of noise at the k'th experiment, which is represented in degrees. As an alternative measure of estimation noises, we can use Eq. (8) by defining

$$g_k := \frac{180 \text{ deg}}{\pi}\frac{1}{N_t}\sum_{j=1}^{N_t} \|\boldsymbol{\eta}_k^{(j)}\|. \tag{10}$$

By changing the orientations of the mockup face, we perform the same experiment $N = 50$ times. Figures 3(a) and 3(b) show the norms of noises, f_k and g_k $(k = 1, \ldots, N)$ described in Eqs. (9) and (10), respectively. The horizontal axes in Fig. 3 represent the index of experiments k. Since f_k is close to g_k, one may choose f_k or g_k as a norm of estimation noises.

5.1.2 *Analysis of error covariance*

From Eq. (5), we can now compute ξ_k, $(k = 1, \ldots, N)$. Figure 3(c) shows the relative angular error

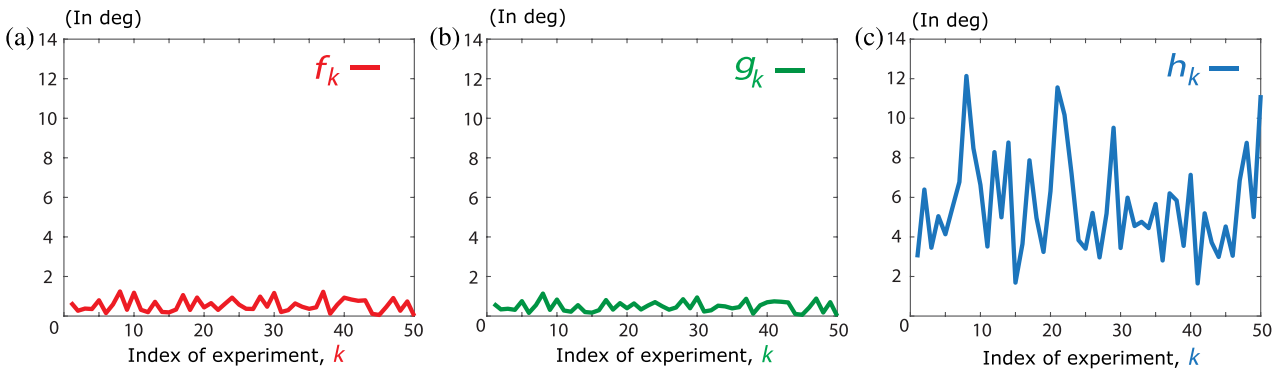

Fig. 3 Experimental results by using the Intel RealSense™ F200 RGB-D camera and the SDK 2015 R5. (a) and (b) Norm of noise and (c) relative angular error.

Table 1 The relative angular error of the head tracker system (Intel RealSense™ F200 camera and the SDK 2015 R5) at the k'th measurement.

	$k=1$	$k=9$	$k=20$	$k=22$	$k=36$	$k=47$
h_k (deg)	2.97	8.48	6.32	10.17	2.81	6.85

$$h_k := \frac{180 \text{ deg}}{\pi} \|\xi_k\|, \tag{11}$$

which is represented in degrees. Recall that $\|\xi_k\|$ is not the estimation error (i.e., $\|\xi_k\| \neq \|\delta \mathbf{G}_k\|$) but represents the relative angular error with respect to the average of error rotations. As derived in Eq. (6), we can compute the error covariance $\mathbf{P}$ from ξ_k, $(k = 1, \ldots, N)$.

Table 1 presents the value of h_k at $k = 1$, 9, 20, 22, 36, and 47. The images of the mockup face corresponding to Table 1 are shown in Fig. 2. From Eqs. (7) and (8), we can obtain $\frac{180 \text{ deg}}{\pi}\epsilon = 5.17$ deg and $\frac{180 \text{ deg}}{\pi}\gamma = 5.62$ deg. As a measure of the uncertainty of estimators, we can choose one from $\frac{180 \text{ deg}}{\pi}\epsilon$ or $\frac{180 \text{ deg}}{\pi}\gamma$.

5.2 *Second Experiment by Using the Intel RealSense™ SR300 RGB-D Camera and the SDK 2016 R2*

By following exactly the same procedure as described in the previous section, we can evaluate the performance of another head tracker system, which is composed of the SR300 camera and the SDK 2016 R2. Figure 4 shows the performance of this head tracker. Table 2 demonstrates that the performance of the head tracker consisting of the SR300 camera and the SDK 2016 R2 is superior to that of their outdated predecessors, i.e., F200 camera and the SDK 2015 R5 in terms of reliability.

Since the proposed method does not compel the person under examination to direct his head toward certain directions, it may be useful when evaluating the reliability of various head trackers.

Table 2 Comparison of the performances of two different head tracker systems.

	The algebraic average of norms of noises		The measure of the uncertainty of estimators	
Head tracker systems	$\frac{1}{N}\sum_{k=1}^{N} f_k$	$\frac{1}{N}\sum_{k=1}^{N} g_k$	$\frac{180 \text{ deg}}{\pi}\epsilon$	$\frac{180 \text{ deg}}{\pi}\gamma$
F200 camera, SDK 2015 R5 (deg)	0.54	0.53	5.17	5.62
SR300 camera, SDK 2016 R2 (deg)	0.11	0.11	4.52	4.84

6 Conclusion

In this paper, a method for evaluating the performance of head orientation trackers by computing the error covariance has been presented. The Schatten 2-norm of a square root of error covariance (or the algebraic average of relative error angles) has been computed as an uncertainty measure of estimators. The merit of the proposed method is that it does not disturb the person under examination by asking him to direct his head toward certain directions. Experimental results using real data have validated the usefulness of our method.

Appendix A: Frobenius Norm and Schatten 2-Norm

The Frobenius norm of a matrix $\mathbf{A} \in \mathbb{R}^{m \times n}$ is defined as $\|\mathbf{A}\|_F := (\sum_{i=1}^{m}\sum_{j=1}^{n} |a_{ij}|^2)^{1/2}$, where a_{ij} denotes the i,j entry of $\mathbf{A}$. It is well known that the value of the Frobenius norm is equal to that of the Schatten 2-norm. This can be proved as follows.[21]

Proposition 1. Suppose the rank of a matrix $\mathbf{A} \in \mathbb{R}^{m \times n}$ is r. Then, $\|\mathbf{A}\|_F = (\sum_{m=1}^{r} s_m^2)^{1/2}$, where $s_1, \ldots, s_r$ denote the singular values of $\mathbf{A}$.

Proof. Let the SVD of $\mathbf{A}$ be given by $\tilde{\mathbf{U}}\Sigma\tilde{\mathbf{V}}^{\mathrm{T}}$, where $\tilde{\mathbf{U}}, \tilde{\mathbf{V}}$ are orthogonal matrices and Σ is a diagonal matrix.

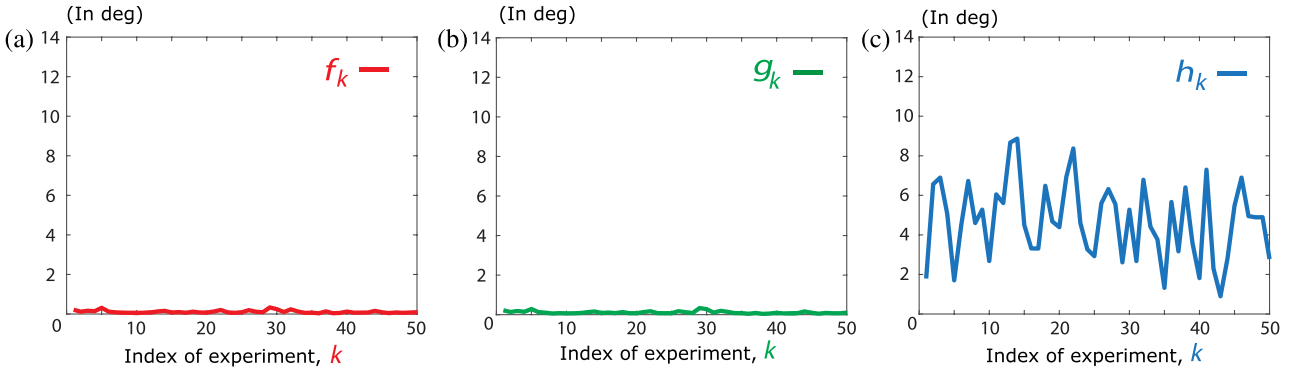

Fig. 4 Experimental results by using the Intel RealSense™ SR300 RGB-D camera and the SDK 2016 R2. (a) and (b) Norm of noise and (c) relative angular error.

Thus, $\|\mathbf{A}\|_F = [\mathrm{tr}(\mathbf{A}^T\mathbf{A})]^{1/2} = [\mathrm{tr}(\tilde{\mathbf{V}}\Sigma^T\Sigma\tilde{\mathbf{V}}^T)]^{1/2}$. Using the matrix trace identity $\mathrm{tr}(\mathbf{CDE}) = \mathrm{tr}(\mathbf{ECD}) = \mathrm{tr}(\mathbf{DEC})$, we have $[\mathrm{tr}(\tilde{\mathbf{V}}\Sigma^T\Sigma\tilde{\mathbf{V}}^T)]^{1/2} = [\mathrm{tr}(\tilde{\mathbf{V}}^T\tilde{\mathbf{V}}\Sigma^T\Sigma)]^{1/2} = [\mathrm{tr}(\Sigma^T\Sigma)]^{1/2} = [\sum_{m=1}^{r} s_m^2]^{1/2}$. Hence, $\|\mathbf{A}\|_F = (\sum_{m=1}^{r} s_m^2)^{1/2}$. □

Acknowledgments

This research was supported by Korea Institute of Science and Technology (KIST) institutional project.

References

1. A. Narayanan, R. M. Kaimal, and K. Bijlani, "Estimation of driver head yaw angle using a generic geometric model," *IEEE Trans. Intell. Transp. Syst.* **17**(12), 3446–3460 (2016).
2. V. Drouard et al., "Robust head-pose estimation based on partially-latent mixture of linear regressions," *IEEE Trans. Image Process.* **26**(3), 1428–1440 (2017).
3. G. Sang et al., "Learning toward practical head pose estimation," *Opt. Eng.* **56**(8), 083104 (2017).
4. E. Murphy-Chutorian and M. M. Trivedi, "Head pose estimation in computer vision: a survey," *IEEE Trans. Pattern Anal. Mach. Intell.* **31**(4), 607–626 (2009).
5. M. Krinidis, N. Nikolaidis, and I. Pitas, "3-D head pose estimation in monocular video sequences using deformable surfaces and radial basis functions," *IEEE Trans. Circuits Syst. Video Technol.* **19**(2), 261–272 (2009).
6. S. J. Lee et al., "Real-time gaze estimator based on driver's head orientation for forward collision warning system," *IEEE Trans. Intell. Transp. Syst.* **12**(1), 254–267 (2011).
7. A. Narayanan, R. M. Kaimal, and K. Bijlani, "Yaw estimation using cylindrical and ellipsoidal face models," *IEEE Trans. Intell. Transp. Syst.* **15**(5), 2308–2320 (2014).
8. F. Vicente et al., "Driver gaze tracking and eyes off the road detection system," *IEEE Trans. Intell. Transp. Syst.* **16**(4), 2014–2027 (2015).
9. S. Li et al., "Real-time head pose tracking with online face template reconstruction," *IEEE Trans. Pattern Anal. Mach. Intell.* **38**(9), 1922–1928 (2016).
10. D. Kang, J. Kim, and S.-K. Kim, "Affine registration of three-dimensional point sets for improving the accuracy of eye position trackers," *Opt. Eng.* **56**(4), 043105 (2017).
11. W. Hoff and T. Vincent, "Analysis of head pose accuracy in augmented reality," *IEEE Trans. Visual Comput. Graphics* **6**(4), 319–334 (2000).
12. G. Fanelli et al., "Random forests for real time 3D face analysis," *Int. J. Comput. Vision* **101**(3), 437–458 (2013).
13. S. Taheri, A. C. Sankaranarayanan, and R. Chellappa, "Joint albedo estimation and pose tracking from video," *IEEE Trans. Pattern Anal. Mach. Intell.* **35**(7), 1674–1689 (2013).
14. F. C. Park and B. J. Martin, "Robot sensor calibration: solving $AX = XB$ on the Euclidean group," *IEEE Trans. Robot. Automat.* **10**(5), 717–721 (1994).
15. J. Park and W.-K. Chung, "Geometric integration on Euclidean group with application to articulated multibody systems," *IEEE Trans. Rob.* **21**(5), 850–863 (2005).
16. Z. Zhang, "A flexible new technique for camera calibration," *IEEE Trans. Pattern Anal. Mach. Intell.* **22**(11), 1330–1334 (2000).
17. R. Hartley et al., "Rotation averaging," *Int. J. Comput. Vision* **103**(3), 267–305 (2013).
18. J. Kwon et al., "A geometric particle filter for template-based visual tracking," *IEEE Trans. Pattern Anal. Mach. Intell.* **36**(4), 625–643 (2014).
19. E. Begelfor and M. Werman, "How to put probabilities on homographies," *IEEE Trans. Pattern Anal. Mach. Intell.* **27**(10), 1666–1670 (2005).
20. T. D. Barfoot and P. T. Furgale, "Associating uncertainty with three dimensional poses for use in estimation problems," *IEEE Trans. Rob.* **30**(3), 679–693 (2014).
21. L. N. Trefethen and D. Bau, *Numerical Linear Algebra*, SIAM, Philadelphia (1997).

Donghoon Kang received his BS and MS degrees in mechanical engineering from Pohang University of Science and Technology, Pohang, Republic of Korea in 1997 and 1999, respectively. Currently, he is working toward his PhD at Seoul National University, Seoul, Republic of Korea. Since 2000, he has been at Korea Institute of Science and Technology, where he is currently a research scientist. His current research interests include signal processing and computer vision.